Available online at www.sciencedirect.com

ScienceDirect

Procedia Structural Integrity 21 (2019) 46–51

Structural Integrity Procedia

www.elsevier.com/locate/procedia

1st International Workshop on Plasticity, Damage and Fracture of Engineering Materials

Formulation and Implementation of a New Porous Plasticity Model

Tuncay Yalçinkaya[a,*], Can Erdoğan[a], Izzet Tarik Tandoğan[a], Alan Cocks[b]

[a]*Department of Aerospace Engineering, Middle East Technical University, Ankara 06800, Turkey*
[b]*Department of Engineering Science, University of Oxford, Parks Road, Oxford, OX1 3PJ, UK*

Abstract

A new rate independent porous plasticity model is proposed for the modeling of ductile damage initiation due to void growth in metallic materials. The model is based on a simple yield description which includes two porosity functions that affect both deviatoric and hydrostatic stress evolution. The current version of the model predicts damage solely due to void growth and it should be extended to include the void initiation and coalescence criteria. The numerical examples study the performance of the developed model for the evolution of porosity through unit cell calculations and for the necking of a uniaxial tensile bar. The preliminary void growth calculations in the unit cell study is acceptable at triaxiality values below 1.

Keywords: porous plasticity, damage, softening;

1. Introducion

It is a well-known fact that the physical mechanism behind the ductile fracture of metals is the micro void nucleation, growth and coalescence. Pores nucleate due to the decohesion of the particle and matrix interface or cracking of the second phase particles and they grow under the effect of plastic deformations of the surrounding matrix (Tvergaard, 1989). Many researchers investigated broadly this phenomenon and developed material models to take into account the influence of void initiation, growth and coelecense in the damage and fracture of metallic materials (eg. McClintock (1968), Rice and Tracey (1969), Gurson (1977),Tvergaard (1981),Tvergaard (1982), Tvergaard and Needleman (1984), Cocks (1989), Benzerga and Leblond (2013)). Gurson (1977) has established the most popular porous plasticity model using upper-bound limit load analysis on spherical and cylindrical voids which was later improved by Tvergaard (1981),Tvergaard (1982) and extended by Tvergaard and Needleman (1984) to include the effects of coalescence of voids which results in a sudden loss of stress carrying capacity. Idea behind these constitutive models is that yield potential of the material is governed by both the deviatoric and hydrostatic stress states together with the effect of void volume fraction.

* Yalçinkaya T. Tel.: +90-312-210-4258 ; fax: +90-312-210-4250.
E-mail address: yalcinka@metu.edu.tr

2452-3216
10.1016/j.prostr.2019.12.085

In this paper, an alternative framework for rate independent porous plasticity is presented to model the ductile damage behavior of metals. Although GTN (Gurson,Tvergaard and Needleman) based models are broadly used and worked on by many researchers and show good agreement with experiments and unit cell calculations, the current formulation is believed to be in a simpler potential form which is easy to implement as well. The model has been motivated by the creep models based on the void growth mechanisms suggested by Cocks (see eg. Cocks (1989)). Proposed model employs two functions of porosity which effect the deviatoric and hydrostatic stresses separately to predict the damage due to void volume fraction increase. Void growth mechanism is associated with the volumetric strains. Porous plasticity model is implemented in finite element solver ABAQUS using using both explicit and implicit user defined material subroutines (VUMAT and UMAT). Unit cell calculations are conducted to address the performance of the model for the modeling of pore evolution under uniaxial loading and for the modeling of damage evolution in necking specimen.

The paper is organized as follows. In section 2, the porous plasticity model is presented briefly with material parameters used in numerical examples. Behavior of the model is compared with unit cell results and the necking example is studied in section 3. Finally the conclusions and the outlook is presented in section 4.

2. Formulation of the porous plasticity model

In this section, the formulation of the porous plasticity model is discussed briefly. Any bold text or symbol in this paper represents a second order tensor ($\boldsymbol{\sigma}$ or $\boldsymbol{\varepsilon}$) and the capital letters (eg. $\mathbb{C}$, $\mathbb{P}$) show fourth order tensors. Proposed rate independent porous plasticity model has the following yield representation in terms of stress, porosity and yield strength. A similar form was suggested by Cocks (1989) for a creep formulation based on void growth mechanism.

$$\phi = \sqrt{\frac{3}{2}\frac{\boldsymbol{\sigma}' : \boldsymbol{\sigma}'}{g_1(p)} + \frac{1}{9}\frac{(tr(\boldsymbol{\sigma}))^2}{g_2(p)}} - \sigma_y \tag{1}$$

where $tr(\boldsymbol{\sigma})$ is the trace and $\boldsymbol{\sigma}'$ is the deviatoric part of the stress tensor ($tr(\boldsymbol{\sigma}) = \boldsymbol{\sigma}_{ii}$, $\boldsymbol{\sigma}' = \boldsymbol{\sigma} - \frac{1}{3}\, tr(\boldsymbol{\sigma})\, \mathbf{1}$). g_1 and g_2 are the functions of void volume fraction p (porosity) and they are currently defined as follows:

$$g_1(p) = \frac{(1-p)^2}{1+\frac{2}{3}p}, \qquad g_2(p) = (ln(\frac{1}{p}))^2. \tag{2}$$

The behavior of porosity functions is illustrated in Fig. 1 together with the shape of yield surface in terms of equivalent and the mean stress,

$$\sigma_{eq} = \sqrt{\frac{3}{2}\boldsymbol{\sigma}' : \boldsymbol{\sigma}'}, \qquad \sigma_m = \frac{1}{3}(tr(\boldsymbol{\sigma})). \tag{3}$$

It can be clearly seen that the yield state depends both on the equivalent von Mises stress and the hydrostatic stress. The proposed porous plasticity model predicts the damage due to solely the void growth with the following pore evolution rule which is obtained from the assumption of incompressible matrix material,

$$\dot{p} = tr(\dot{\boldsymbol{\varepsilon}})(1-p). \tag{4}$$

The evolution of the plastic strain is governed by the following associative plastic flow rule,

$$\begin{aligned} \dot{\boldsymbol{\varepsilon}}^p &= \lambda \frac{\partial \phi}{\partial \boldsymbol{\sigma}} \\ \dot{\boldsymbol{\varepsilon}}^p &= \lambda \left(\frac{3}{2}\frac{\boldsymbol{\sigma}'}{\overline{\sigma} g_1} + \frac{1}{9}\frac{tr(\boldsymbol{\sigma})}{\overline{\sigma} g_2}\mathbf{1} \right), \end{aligned} \tag{5}$$

where $\overline{\sigma}$ is the effective stress is $\overline{\sigma} = \sqrt{\frac{3}{2}\frac{\boldsymbol{\sigma}':\boldsymbol{\sigma}'}{g_1(p)} + \frac{1}{9}\frac{(tr(\boldsymbol{\sigma}))^2}{g_2(p)}}$.

The plasticity model is implemented in ABAQUS as user defined material subroutines UMAT and VUMAT for implicit and explicit finite element applications accordingly, employing the classical radial return algorithm. Since the derivation of the consistent tangent modulus is quite complicated for the UMAT subroutine, numerical tangent mod-

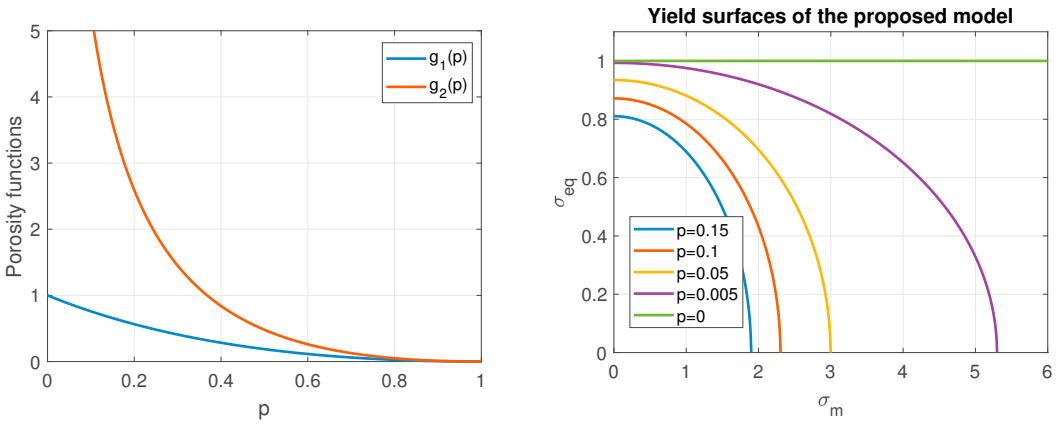

Fig. 1. Evolution of the porosity functions(left), yield surface representation of the proposed model at different porosity levels(right)

ulus is implemented using the perturbation method, where 6 components of the strain tensor is perturbed separately with a very small value (10^{-10}). The stress tensor is calculated for each perturbation state and then modulus is computed from $\mathbb{C}_{n+1} = \frac{\Delta\boldsymbol{\sigma}_{n+1}}{\Delta\boldsymbol{\varepsilon}_{n+1}}$. Note that, explicit finite element solver with VUMAT does not require a tangent modulus tensor.

The following Voce type non-linear hardening relation is employed in the model (see Simo and Hughes (2000)) to describe the isotropic hardening phenomenon in the FEM calculations,

$$\sigma_y = y_0 + (y_\infty - y_0)(1 - exp(-\omega\alpha)) \tag{6}$$

where y_0 is the initial yield stress, y_∞ is the saturated yield stress, ω is saturation parameter, and α is accumulated plastic strain ($\alpha = \int_0^t \|\dot{\boldsymbol{\varepsilon}}^p(\tau)\| d\tau$) which is an internal variable of the constitutive model. The material parameters are presented in table 1, which represent a moderate strength steel with a non linear hardening behavior.

y_0	y_∞	ω	E	μ
200 [MPa]	400 [MPa]	10	210000 [MPa]	0.3

Table 1. Material parameters

3. Numerical examples

In this section, performance of the model is illustrated through two different numerical examples. The preliminary results on the evolution of porosity through unit cell calculations and the necking of a uniaxial tensile specimen are presented.

3.1. Unit cell calculations

It has been shown by many researchers that initiation and the growth of micro voids in metallic materials is the main failure mechanism for the ductile damage and fracture, which is directly related to the stress triaxiality of the matrix material (eg. Hancock and Mackenzie (1976), Hancock and Brown (1983)). Computational unit cell models has been a useful tool for investigation of the effect of triaxiality on the void growth (eg. Needleman (1972), Koplik and Needleman (1988), Pardoen and Hutchinson (2000), Scheyvaerts et al. (2010)). In order to test the porosity and damage evolution of the developed model, unit cell calculations are performed on a 1/8 cube using C3D8 elements in Abaqus. Several methods for unit cell calculations with constant triaxiality has been developed (see e.g. Lin et al. (2006) for axisymmetric cell models, Tekoglu (2014) for 3-D cells). In the example here the triaxiality is kept constant by controlling the ratio of applied tractions on the surfaces of the unit cell. Throughout the deformation due to the

evolving plasticity the load carrying capacity might decrease, therefore Riks algorithm in Abaqus is used to control the applied tractions.

Finite element model of the unit cell with boundary conditions can be seen from the Fig. 2. As discussed in Lin

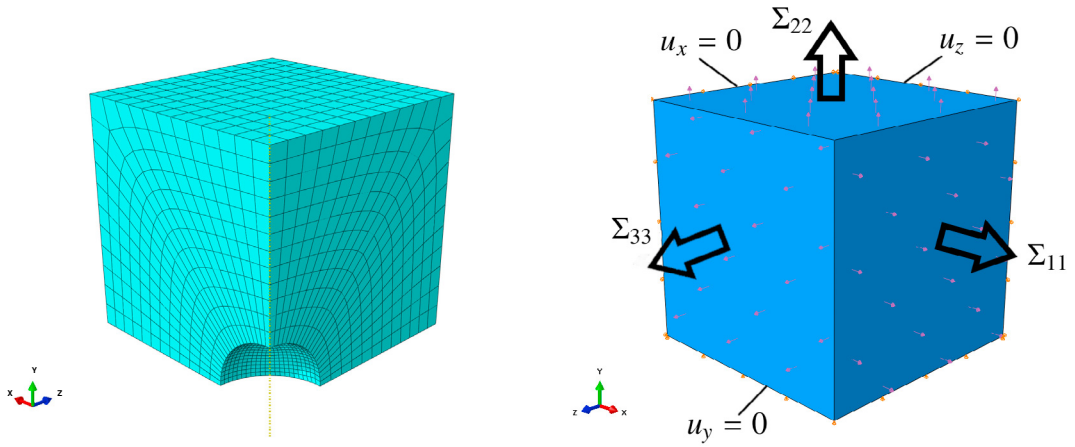

Fig. 2. Finite element model of the unit cell with initial void fraction of 0.01% (left), boundary conditions of both unit cell and the unit cube used for porous model (right)

et al. (2006)), applying traction to a heterogeneous cell causes uneven deformations at the cell boundaries. To prevent this, all nodes of the outer boundary of the cell should have the same displacement in the normal direction of the surface. This condition is accomplished by equating the corresponding displacement component of one node to all other nodes on the same surface. For the faces adjacent to the void, symmetric boundary condition is applied.

The pore volume evolution is calculated through J2 plasticity model for the unit cell and it is compared with the pore evolution obtained through the developed porous plasticity model for different triaxiality values ($T = 0.35,\ 1,\ 2$) in Fig. 3 under same boundary conditions and hardening rule.

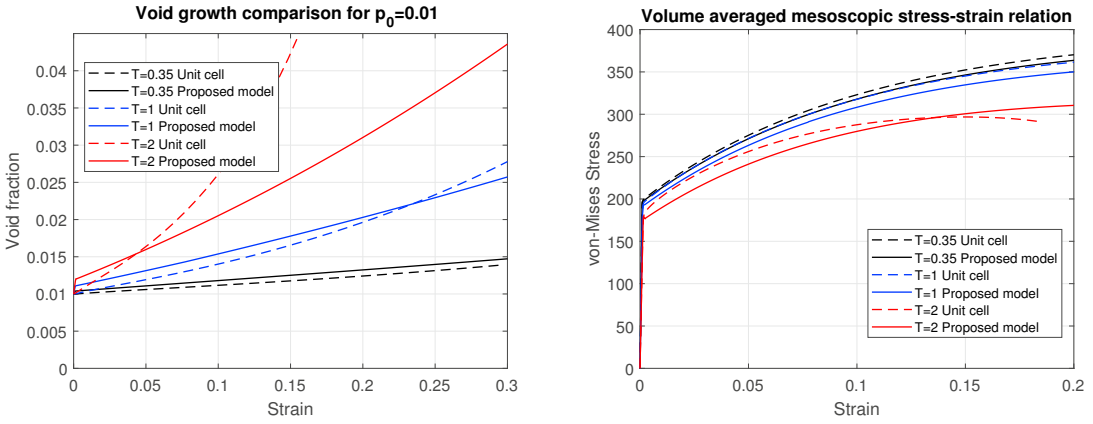

Fig. 3. Void growth comparison for different triaxiality values at P_0=0.01 (left), volume averaged stress-strain response of unit cell calculations and proposed porous plasticity model (right)

The preliminary results show that at low triaxialities the model behavior is acceptable compared to the unit cell results. However, for triaxialities higher than 1, void growth deviates from the unit cell calculations. The proposed model underpredicts the effect of high stress triaxiality in pore growth. Moreover, it can be seen that, elastic deformation causes a sharp increase in the pore fraction especially at high triaxialities which is not observed in the unit cell calculations and in the literature (see e.g. Koplik and Needleman (1988), Pardoen and Hutchinson (2000)). Therefore, this behavior should be eliminated from the proposed model.

Volume averaged stress-strain relations can be seen in the Fig. 3. Averaged stresses drop with the increasing triaxiality for both unit cell model and porous plasticity model. Porous plasticity model gives slightly less stress compared to unit cell model. The difference between the unit cell and the proposed model increases as triaxiality increase.

3.2. Necking simulations

Tensile test on a round specimen is extensively used for understanding the ductile damage and fracture mechanisms. At the necking region, due to high hydrostatic stresses, voids grow and coalesce which leads to fracture of the specimen. To test the model, a round bar with a length of 100 mm is deformed in uniaxial tension using explicit finite element solver. The tensile bar is hold in all degrees of freedom at one end and displacement is applied at the other end. In order to initiate necking, middle section of the specimen is slightly narrowed.

In the Fig. 4, von Mises stress and porosity distributions are shown. It can be seen that at the center of the specimen, where the porosity is highest, stress carrying capacity drops as expected. Note that figures are plotted at the state when the maximum porosity value reaches to $p = 0.1$.

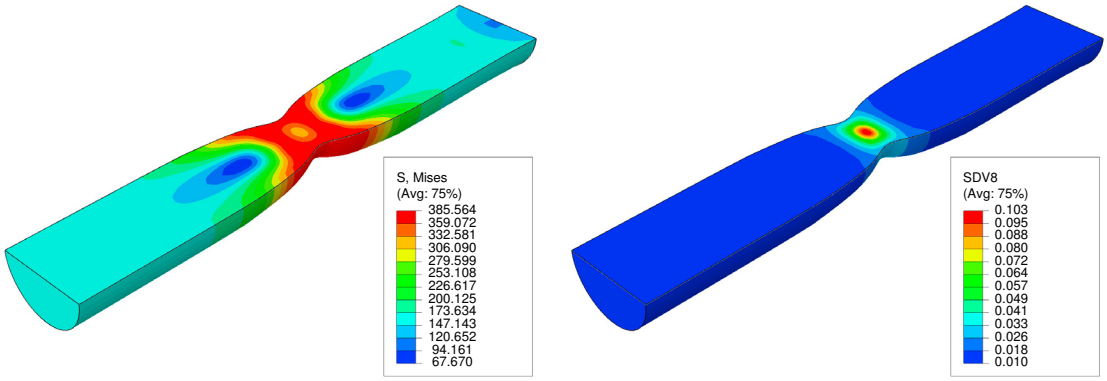

Fig. 4. Necking simulation results at inital porosity of p0 = 0:01: von Mises stress with cut view (left) and porosity distribution (right)

The left part of Fig. 5 shows the engineering stress-strain response obtained from the necking specimen for different initial void volume fractions (porosity). It can be seen that higher initial porosity results in lower maximum stress and the failure strain value. Moreover, the difference between the classical von-Mises plasticity (J2 plasticty) and the proposed model can be observed. With the porous model, the stress carrying capacity is lower and fracture occurs earlier. Note that, although the suggested model predicts the damage only due to void growth, it is possible to achieve failure but at unrealistically high strain and porosity values. Therefore, a simulation with material point deletion, controlled with porosity, is shown as well in the same figure to simulate a more realistic failure behavior using VUMAT (see (Abaqus, 2014) for the details of material point deletion).

The porosity evolution in the necking specimen at the middle of necking region where the void growth is the highest can be seen at the right part of Fig. 5. Sudden increase of the void volume fraction is observed after the strain value of 0.18, at porosity of 0.2, which leads to a rapid loss of load carrying capacity at the necking region. The analysis done with the material point deletion feature can be seen in the same figure where the maximum porosity is limited to 0.1.

4. Concluding remarks

In this paper, the preliminary results of a recently developed rate independent porous plasticity model are presented. The authors aim here to provide a simpler alternative to the existing porous plasticity models. The current version of the model predicts only void growth and the related damage due to incorporated porosity functions. It does not have any void nucleation or coalescence criteria at the moment. The unit cell calculations show that the model under predicts the void growth rate at high stress triaxiality states. The functional form of the porosity functions will be tuned according to the unit cell calculations to obtain more realistic representation of the damage and to conduct

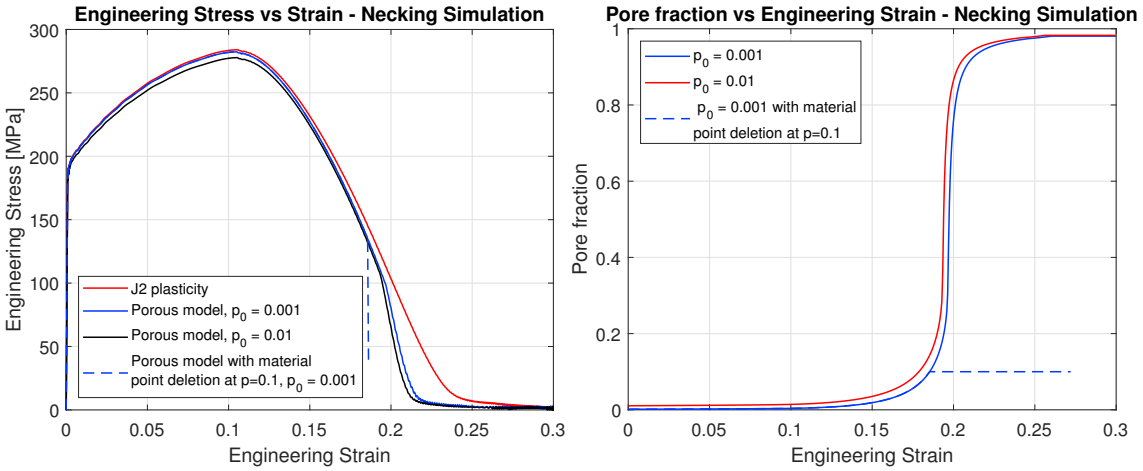

Fig. 5. Engineering stress-strain response of the necking specimen through both J2 and porous plasticity models at two different initial pore fractions (left), evolution of the porosity at the middle of the necking region (right)

experimental comparison. The simple representation of the model and the lack of material parameters offer a good potential for the use in ductile damage and fracture simulations.

Acknowledgements

Tuncay Yalçinkaya gratefully acknowledges the support by the Scientific and Technological Research Council of Turkey (TÜBİTAK) under the 3501 Programme (Grant No. 117M106).

References

Abaqus, 2014. The Abaqus documentation collection, version 6.14. Dassault Systèmes, Providence, Rhode Island .

Benzerga, A.A., Leblond, J.B., 2013. Effective Yield Criterion Accounting for Microvoid Coalescence. Journal of Applied Mechanics 81.

Cocks, A., 1989. Inelastic deformation of porous materials. Journal of the Mechanics and Physics of Solids 37, 693 – 715.

Gurson, A.L., 1977. Continuum Theory of Ductile Rupture by Void Nucleation and Growth: Part I—Yield Criteria and Flow Rules for Porous Ductile Media. Journal of Engineering Materials and Technology 99, 2–15.

Hancock, J., Brown, D., 1983. On the role of strain and stress state in ductile failure. Journal of the Mechanics and Physics of Solids 31, 1 – 24.

Hancock, J., Mackenzie, A., 1976. On the mechanisms of ductile failure in high-strength steels subjected to multi-axial stress-states. Journal of the Mechanics and Physics of Solids 24, 147 – 160.

Koplik, J., Needleman, A., 1988. Void growth and coalescence in porous plastic solids. International Journal of Solids and Structures 24, 835 – 853.

Lin, R., Steglich, D., Brocks, W., Betten, J., 2006. Performing rve calculations under constant stress triaxiality for monotonous and cyclic loading. International Journal for Numerical Methods in Engineering 66, 1331 – 1360.

McClintock, F.A., 1968. A Criterion for Ductile Fracture by the Growth of Holes. Journal of Applied Mechanics 35, 363–371.

Needleman, A., 1972. Void Growth in an Elastic-Plastic Medium. Journal of Applied Mechanics 39, 964–970.

Pardoen, T., Hutchinson, J., 2000. An extended model for void growth and coalescence. Journal of the Mechanics and Physics of Solids 48, 2467 – 2512.

Rice, J., Tracey, D., 1969. On the ductile enlargement of voids in triaxial stress fields. Journal of the Mechanics and Physics of Solids 17, 201 – 217.

Scheyvaerts, F., Pardoen, T., Onck, P., 2010. A new model for void coalescence by internal necking. International Journal of Damage Mechanics 19, 95–126.

Simo, J., Hughes, T., 2000. Computational Inelasticity. Interdisciplinary Applied Mathematics, Springer New York.

Tekoglu, C., 2014. Representative volume element calculations under constant stress triaxiality, lode parameter, and shear ratio. International Journal of Solids and Structures 51, 4544 – 4553.

Tvergaard, V., 1981. Influence of voids on shear band instabilities under plane strain conditions. International Journal of Fracture 17, 389–407.

Tvergaard, V., 1982. On localization in ductile materials containing spherical voids. International Journal of Fracture 18, 237–252.

Tvergaard, V., 1989. Material failure by void growth to coalescence, Elsevier. volume 27 of *Advances in Applied Mechanics*, pp. 83 – 151.

Tvergaard, V., Needleman, A., 1984. Analysis of the cup-cone fracture in a round tensile bar. Acta Metallurgica 32, 157 – 169.